Stability of Voltage and Frequency Control in Distributed Generation Based on Parallel-Connected Converters Feeding Constant Power Loads

Per Karlsson, Johan Björnstedt and Magnus Ström
Department of Industrial Electrical Engineering and Automation, Lund University
Box 118, SE-221 00
Lund, Sweden
Phone: +46 46 222 92 90
Fax: +46 46 14 21 14
e-mail: per.karlsson@iea.lth.se
URL: http://www.iea.lth.se

Keywords

Converter control, Distribution of electrical energy, Distributed power, Renewable energy systems

Acknowledgements

The ambition to merge the fields of power electronics and power engineering at the Department of Industrial Electrical Engineering and Automation at Lund University is greatly acknowledged. Especially, Gustaf Olsson and Olof Samuelsson are acknowledged for their efforts. Lars Gertmar is also acknowledged for the fruitful discussions and being a never-ending source of inspiration.

Abstract

In this paper stability and dynamic properties of voltage and frequency droop control of power electronic converters are investigated for a distributed generation system. Droop control is utilized to share active and reactive power among the source converters. The voltage and frequency controllers are designed so that stand-alone converter operation feeding constant power loads performs satisfactory. These controllers are adapted to mimic the behaviour of present rotating generators connected directly to the power system, for seam-less transfer between island and grid-connected modes of operation. Small-signal and switch-mode, time-domain simulation results of a three-converter distributed generation system facilitating stand-alone operation verify the operation. Experimental results of a three-converter stand-alone system are also included for verification.

Introduction

In this paper, AC bus voltage control and its stationary and dynamic behaviour are investigated. Voltage and frequency control is local in the sense that high-speed communication between the sources is not used and therefore droop control [1] is utilized to achieve load-sharing. The derived droop control scheme is stable both in the case of normal operation, i.e. when connected to a strong AC network or when rotating sources are connected to the power system, but also in the case when only power electronic converters are connected to the power system both as sources and loads. Usually, two separate control modes need to be implemented [2], but here the same is used for both cases. In the most extreme case the loads also operate in constant power mode, which is covered in the analysis. The local distributed power system is shown in Fig. 1.

This paper treats current control, frequency estimation and droop control for the converters of the system shown in Fig. 1. The presented theory is verified in simulations and experiments. Suitable controller and filter parameters are found from small-signal analysis in MATLAB^{TM}. A switch-mode simulation model implemented in DYMOLA^{TM} is then used to verify the controller parameters. The dynamic properties, in terms of step-responses, are compared for the two simulation environments. To fully verify the behaviour of the system an experimental setup is also implemented.

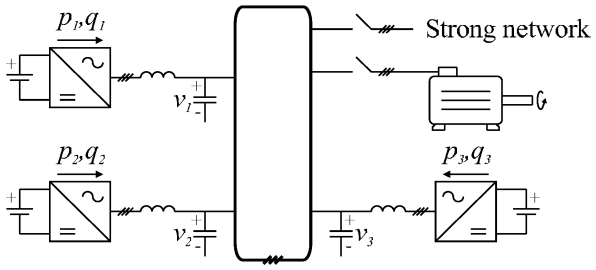

Fig. 1: The investigated distributed power system. Note that stable operation of the system is required in all operating modes, i.e. with or without a strong AC network or generators connected to the system. Units 1 and 2 operate as sources and unit 3 as load.

Voltage and frequency droop control

In regular droop control utilized for rotating generators, the active power reference is calculated based on the frequency error and the reactive power reference is calculated based on the voltage error, see Fig. 2. In stationary operation this means that active power is shared as intended since the frequency is the same in the power system. However, reactive power is not necessarily shared as intended since the voltage is different at different locations of the power system [3].

In the case of droop control of a local AC power system where only converters are connected both as sources and loads the regular droop functions are not directly applicable. Firstly, for a power system based on rotating generators, frequency and active power is closely interconnected since a load power increase implies that the load torque increases without a corresponding increase in the turbine torque which means that the rotational speed, and thereby the frequency, decreases. The frequency droop acts in such a way that the turbine torque is increased for decreasing frequency so that a new stable operating point is reached. A corresponding relationship is true for voltage control through reactive power generation. In most cases, voltage and frequency droop controllers for power electronic converters intended for distributed generation mimics this behaviour [4]. Secondly, for the grid voltage to be sinusoidal at the specified fundamental, AC side capacitors must be added. For a simple capacitive network with only power electronic converters connected (Fig. 1 with total capacitance C)

$$\begin{cases} \dfrac{dv_d}{dt} = \omega v_q + \dfrac{1}{C} i_{1d} + \dfrac{1}{C} i_{2d} + \dfrac{1}{C} i_{3d} \\ \dfrac{dv_q}{dt} = -\omega v_d + \dfrac{1}{C} i_{1q} + \dfrac{1}{C} i_{2q} + \dfrac{1}{C} i_{3q} \end{cases} \tag{1}$$

If the reference direction of the rotating coordinate system (dq) is selected so that $\vec{v} = v_d + jv_q = jv_q$ then the receiving end power is expressed as $\vec{s}_3 = p_3 + jq_3 = v_q i_{3q} + jv_q i_{3d}$ where i_3 is the inductor current. This means that if the active load power increases (p_3 and i_{3q} negative) without a corresponding increase in the active power supplied by the sources, v_q must decrease. This implies that, for transients at least, active power is controlled by voltage or in other words the droop function giving the sending end active power reference should be based on the voltage error. If the reactive load power increases (q_3 and i_{3d} negative) without a corresponding increase in the reactive power supplied by the sources, ωv_q must increase. Since v_q is related to active power this is solved by increasing only ω to achieve decoupling. For transients at least, reactive power is controlled by frequency, i.e. the droop function yielding the sending end reactive power reference should be based on the negative frequency error. Consequently, the droop functions giving the active and reactive power references, p_s^* and q_s^*, should be (index s denotes source converter, i.e. units 1 and 2 here)

$$\begin{cases} p_s^* = K_v \left(v^{ref} - v_q \right) \\ q_s^* = -K_\omega \left(\omega^{ref} - \omega \right) \end{cases} \tag{2}$$

These droop functions are also shown in Fig. 2. However, it is of course important that load-sharing is achieved also in non-islanded operation, i.e. when the system is connected to a strong power grid or when rotating generators are included in the scheme. This is not true for source converter references according to equation (2) since the droop functions of rotating power sources are

$$\begin{cases} p_s^* = K_\omega\left(\omega^{ref} - \omega\right) \\ q_s^* = K_v\left(v^{ref} - v_q\right) \end{cases} \tag{3}$$

Even worse, if a generator with droop functions according to (3) is connected to a converter system where the sources operate according to droop functions specified by (2), the resulting system is unstable, which is also found from an inspection of the pole-zero maps and Bode-diagrams of the small-signal model of such a system. However, the resulting system is stable if both source converters and rotating generators operate according to the droop functions in (3). Therefore, one could try to detect, from system behaviour, if there are rotating sources present and select appropriate droop functions from the result. The method selected here is to modify the droop functions of the source converters so that for transients they operate according to (2) but in steady-state the source converters operate as specified by (3). In the next section the derivation of the additional functionality needed to accomplish this task in a converter digital signal processor (DSP) is presented.

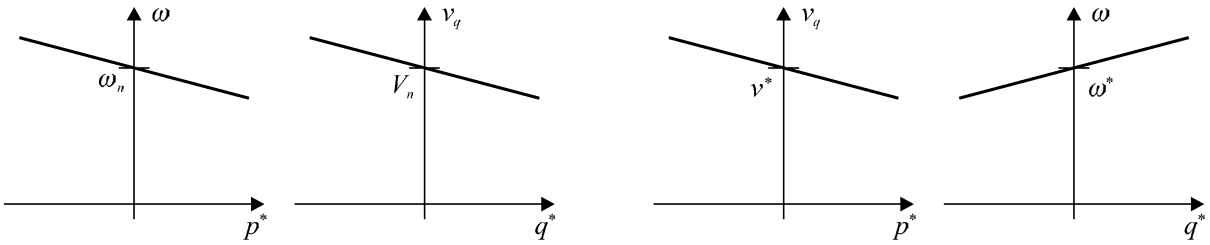

Fig. 2: Regular droop functions (*left*) and transient droop functions (*right*). Here the regular droop functions are also referred to as the steady-state droop functions. Note that here $\omega^{ref} = \omega_n$ and $v^{ref} = V_n$ for the steady-state droop functions according to (3) and $\omega^{ref} = \omega^*$ and $v^{ref} = v^*$ for the transient droop functions according to (2).

In [5] a related investigation is performed. However, in [5] the focus is on the need of different droop functions for different types of grids. In [5] it is found that for high voltage (mainly inductive) grids the regular droop functions can be used also for distributed generation systems. For low voltage (mainly resistive) grids, so-called opposite droop functions could be used instead but the regular droop functions are advantageous for compatibility reasons [5]. Also, in [5] there is no distinction between transient and steady-state droop functions which may be due to the fact that frequency is not estimated. Instead, the frequency is obtained from the inverse droop characteristic, which means that the actual active output power is used together with the droop function to determine the frequency.

Converter control

The converters are equipped with DSPs where the controller algorithms are running. Vector current control is often utilized for modern high performance voltage source converters (VSCs), see Fig. 3, and is discussed first in this section. In this application the angular position and frequency also need to be estimated, which is also discussed. Last in this section, the actual implementation of the modified droop controllers is presented and suitable converter and controller parameters discussed.

Current control

Each converter in the distributed system is equipped with a vector current controller (Fig. 3). The current controller of each converter is implemented in the rotating *dq*-frame and forms a proportional-integral (PI) controller with feed-forward of the AC side voltage.

 ISBN : 90-75815-08-5

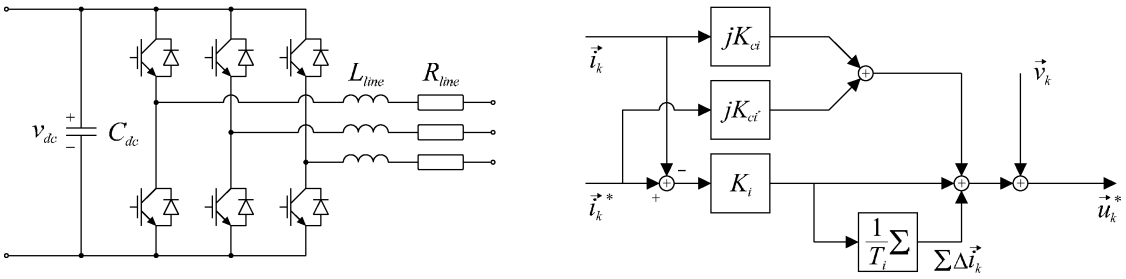

Fig. 3: Converter (*left*) and converter current controller (*right*).

The output of the current controller is a converter terminal voltage reference vector

$$\vec{u}_k^* = K_i\left(\left(\vec{i}_k^* - \vec{i}_k\right) + \sum\Delta\vec{i}_k\right) + K_r\vec{i}_k + jK_{ci}\vec{i}_k + jK_{ci^*}\vec{i}_k^* + \vec{v}_k \tag{4}$$

which is fed to the pulse width modulator. The integral part is updated according to

$$\sum\Delta\vec{i}_{k+1} = \sum\Delta\vec{i}_k + \frac{K_i}{T_i}\left(\vec{i}_k^* - \vec{i}_k\right) \tag{5}$$

where $\vec{i}_k$ is the actual and $\vec{i}_k^*$ the reference current vector at sample k. The parameters of the current controller are set to $K_i = k_i\left(\left(L/T_s\right) + \left(R/2\right)\right)$, $K_i/T_i = k_i R$ and $K_{ci} = K_{ci^*} = \omega_n L/2$, where $L = L_{line}$ and $R = R_{line}$ are the inductance and resistance of the filter inductor (Fig. 3), T_s the sampling interval and ω_n the nominal fundamental frequency of the power system. Note that $k_i = 1$ corresponds to dead-beat response, neglecting the calculation time delay of the DSP. On the contrary to the current controller analyzed in [6] the current controller implemented here is not equipped with a Smith-predictor.

This controller is implemented in the DYMOLA™ switch-mode simulation model. For the small-signal analysis in MATLAB™ the current controller including the inductive output filter is modeled in the same manner as in [6], i.e. its state-space model is derived for different controller gains. The Bode-diagrams for current reference to actual current are shown in Fig. 4.

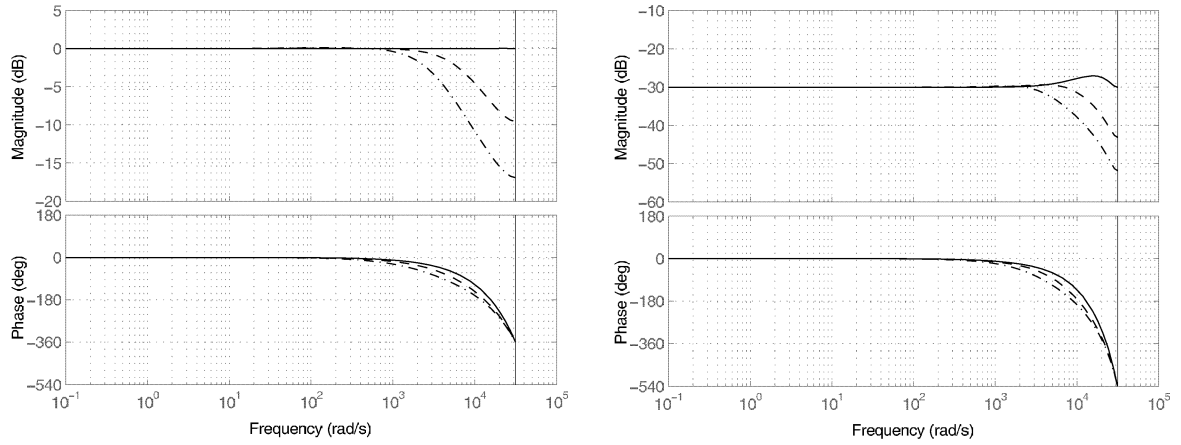

Fig. 4: Bode-diagrams of the transfer functions from i_q^* to i_q (*left*) and i_d^* to i_q (*right*) for k_i=1.0 (solid), k_i=0.5 (dashed) and k_i=0.25 (dash-dotted).

Angular position and frequency estimation

The angular frequency needs to be estimated since the active power control of rotating generators in general is based on the frequency error and the power electronic generators should mimic this behaviour to adapt to the present power system. The angular position needs to be estimated for the vector transformation to *dq*-coordinates utilized in the current controller. In [7], position and speed

estimators are developed for permanent magnet synchronous machines. The same type of estimators can be used also here. The angular position is estimated from

$$\hat{\theta}_{k+1} = \hat{\theta}_k + T_s\hat{\omega}_k + 2\rho_\omega T_s\left(\Delta\hat{\theta}\right) = \hat{\theta}_k + T_s\hat{\omega}_k + \frac{2\rho_\omega T_s}{V_n}\cdot\left(-u_{d,k} + Ri^*_{d,k} - \hat{\omega}_k Li^*_{q,k}\right) \tag{6}$$

and the angular speed is estimated from

$$\hat{\omega}_{k+1} = \hat{\omega}_k + \rho_\omega^2 T_s\left(\Delta\hat{\theta}\right) = \hat{\omega}_k + \frac{\rho_\omega^2 T_s}{V_n}\cdot\left(-u_{d,k} + Ri^*_{d,k} - \hat{\omega}_k Li^*_{q,k}\right) \tag{7}$$

where ρ_ω is the double pole of the speed/position estimator [7] and V_n is the nominal AC side voltage. In the following ω is used instead of $\hat{\omega}$ for the estimated frequency for reasons of simplicity.

Implementation of the droop functions

The transient droop functions operate on the estimated angular frequency as specified above and the low-pass filtered magnitude of the voltage vector of the output filter capacitor calculated from

$$v_{qf,k+1} = \left(1 - T_s\rho_{vq}\right)v_{qf,k} + \left(T_s\rho_{vq}\right)v_{q,k} \tag{8}$$

Therefore, the transient droop functions give the active and reactive power references according to

$$\begin{cases} p^*_k = K_{vt}\cdot\left(v^*_q - v_{qf,k}\right) \\ q^*_k = -K_{\omega t}\cdot\left(\omega^* - \omega_k\right) \end{cases} \tag{9}$$

These references are transformed to current references by

$$\begin{cases} i^*_{d,k} = q^*_k / v_{qinvf,k} \\ i^*_{q,k} = p^*_k / v_{qinvf,k} \end{cases} \tag{10}$$

i.e. the power references are divided by another low-pass filtered version of the output filter capacitor voltage calculated from

$$v_{qinvf,k+1} = \left(1 - T_s\rho_{vqinv}\right)v_{qinvf,k} + \left(T_s\rho_{vqinv}\right)v_{q,k} \tag{11}$$

To fulfil that the steady-state droop functions exhibit the same properties as the ones utilized in the present power system, i.e. depend on frequency and voltage according to (3), the voltage and angular frequency references utilized in (9) are calculated from

$$\begin{cases} v^*_{q,k} = v_{qf2,k} + \dfrac{K_{\omega s}}{K_{vt}}\cdot\left(\omega_n - \omega_{f2,k}\right) \\ \omega^*_k = \omega_{f2,k} - \dfrac{K_{vs}}{K_{\omega t}}\cdot\left(V_n - v_{qf2,k}\right) \end{cases} \tag{12}$$

where a new set of variables are used, v_{qf2} and ω_{f2}, which are calculated according to

$$v_{qf2,k+1} = \left(1 - T_s\rho_{vq2}\right)v_{qf2,k} + \left(T_s\rho_{vq2}\right)v_{q,k} \tag{13}$$

$$\omega_{f2,k+1} = \left(1 - T_s\rho_{\omega 2}\right)\omega_{f2,k} + \left(T_s\rho_{\omega 2}\right)\omega_k \tag{14}$$

Note that $K_{\omega t}$, $K_{\omega s}$, K_{vt} and K_{vs} are all positive. Also note that $\rho_\omega > \rho_{\omega 2}$ and $\rho_{vq} > \rho_{vq2} > \rho_{vqinv}$.

Converter current controller parameters

The parameters of the distributed power system and converters are adapted to the intended experimental setup. The nominal AC side voltage is low, $V_n = V_{LL} = 145$ V, since the distributed power system could be connected to the 400 V grid of the laboratory via a 400/145 V transformer. The rated fundamental frequency is $f_n = \omega_n/2\cdot\pi = 50$ Hz and therefore the natural frequency of the LC-circuit formed by the converter output inductors and the capacitors is set to 500 Hz, i.e. one decade higher than the fundamental frequency. If the DC link voltage of the converters is equal ($V_{dc} = 270$ V) and the output filter inductance of each converter is inversely proportional to its rated power, then the per unit (pu) converter output current ripple is equal. Therefore, the output filter capacitance should be proportional to the rated power. The switching frequency of the converters connected to the power system should ideally be at least one decade higher than the natural frequency of the converter output LC-filters, i.e. $f_{sw} = 5000$ Hz. In high power installations, a lower switching frequency is often necessary and therefore $f_{sw} = 3000$ Hz is also investigated. Since the DYMOLA™ model, but not the MATLAB™ model, is implemented in switch-mode, sampling frequency $f_s = 2\cdot f_{sw}$ is used in the following. The droop functions are specified by the gains $K_{\omega t} = K_{\omega s} = S_n/\omega_n\cdot\delta_\omega$ and $K_{vt} = K_{vs} = S_n/V_n\cdot\delta_v$ where the relative frequency and voltage errors at rated power, S_n, are $\delta_\omega = 0.005$ and $\delta_v = 0.04$. The filters for the droop functions of each source converter have the parameters $\rho_{vq} = 2\cdot\pi\cdot 4.0$ rad/s, $\rho_{vqinv} = 2\cdot\pi\cdot 0.5$ rad/s, $\rho_\omega = 2\cdot\pi\cdot 5.35$ rad/s, $\rho_{vq2} = 2\cdot\pi\cdot 1.0$ rad/s and $\rho_{\omega 2} = 2\cdot\pi\cdot 5.0$ rad/s.

Simulation results

Each cable segment between the converters (Fig. 1) is modeled as being resistive and inductive in the simulation model. Two reactance-to-resistance ratios (X/R) are investigated, 0.1 and 10. In both cases the total impedance of each cable segment is $Z = 0.1$ Ω per phase. Two converters operate as sources (units 1 and 2) controlling the system frequency and voltage. One converter acts as load (unit 3) consuming active and reactive power. The converters (1-3) have rated power 4500 VA, 3000 VA and 7500 VA. To obtain the same per unit current ripple, the AC side filter inductors have inductance 5.0 mH, 7.5 mH and 3.0 mH. The L/R time constant of the filter inductors is 0.1 s. The AC side capacitors are 20 μF, 14 μF and 35 μF with equivalent series resistance (ESR) equal to 20.0 mΩ independent of capacitance. The Bode-diagrams from load converter output power to unit 1 (source) converter AC side voltage and estimated AC side angular frequency, for the three-converter stand-alone system, are shown in Fig. 5. For low frequencies, i.e. in steady-state, active power is correlated with estimated angular frequency and reactive power with AC side voltage, i.e. the system behaviour corresponds to the desired steady-state droop functions (3). For high frequencies, the system behaves according to the transient droop functions (2). The pole-map of this system is shown in Fig. 6.

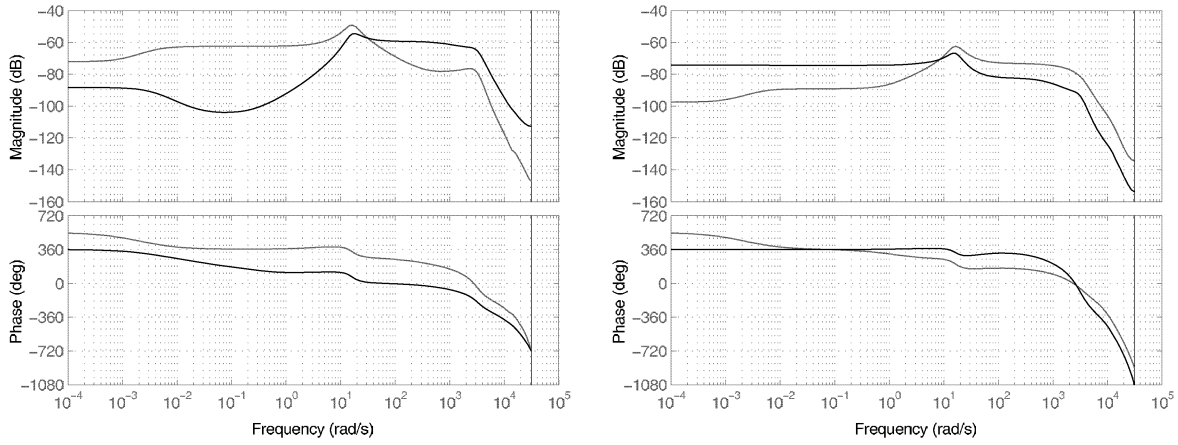

Fig. 5: Bode-diagrams of the transfer functions from p_3^* (*black*) and q_3^* (*grey*) to v_{1qf} (*left*) and ω_1 (*right*) for $k_i = 0.5$ and $f_s = 10.0$ kHz for all three converters. The impedance of the cable segments between the three converters is $Z = 0.1$ Ω and $X/R = 0.1$ each. Note that v_{1qf} is the low-pass filtered AC side voltage and ω_1 is the estimated AC side frequency of unit 1.

 ISBN : 90-75815-08-5

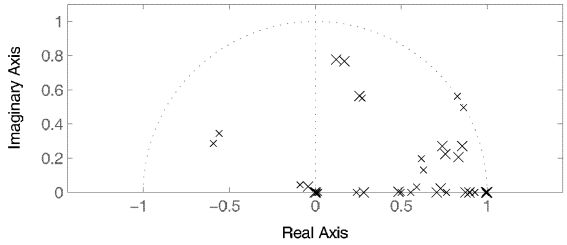

Fig. 6: Location of the poles of the three-converter system in the case of a converter sampling frequency of 10.0 kHz (large markings) and 6.0 kHz (small markings). In this case, the cable segments have a reactance-to-resistance ratio of $X/R=0.1$, i.e. the system is resistive.

From the pole-map in Fig. 6, it could be concluded that proper selection of converter sampling frequency is essential for system stability. The DYMOLA™ switch-mode simulation results, presented later in this section, indicate that there are no stability problems for the investigated sampling frequencies. Instead, it is believed that the MATLAB™ small-signal model is subject to numerical problems. This conclusion is drawn as a result of the high order of the system, 45, and also from the fact that anti-aliasing filters are not included in the MATLAB™ state-space system but are implemented in the DYMOLA™ switch-mode model. In the switch-mode simulations, the active power drawn from the local system by the converter operating as load, i.e. unit 3, is increased by 0.5 pu (unit base) at $t=1.0$ s and the reactive power drawn from the system is increased by 0.5 pu (unit base) at $t=2.0$ s. Note that power is defined as positive flowing into the system (Fig. 1). The switch-mode simulation results for the three-converter stand-alone system are shown in Fig. 7.

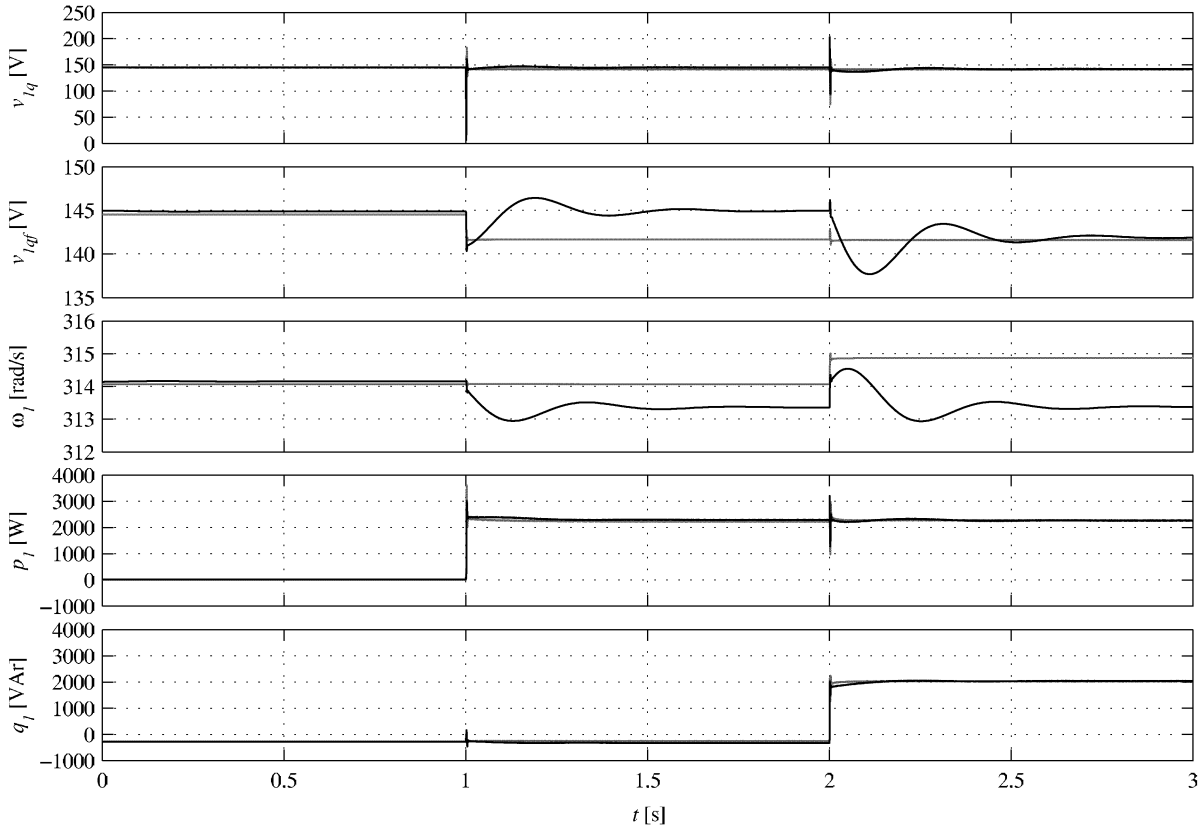

Fig. 7: Switch-mode simulation results for unit 1 (source) in the case of a load converter active power reference (p_3^*) increase of -0.5 pu (-3750 W) at $t=1.0$ s and a load converter reactive power reference (q_3^*) increase of -0.5 pu (-3750 VAr) at $t=2.0$ s. The black traces are for the case with both transient (2) and steady-state (3) droop functions implemented in the source converters and the grey traces are for the case with only transient droop functions (2).

According to the previous discussions, the droop functions specified by (2) should behave satisfactory since this is a purely converter based local distribution system. However, since the system should operate satisfactory also in the case of other sources, e.g. rotating generators, the steady-state droop functions should operate according to (3). In Fig. 7 it is shown that proper operation is obtained both in the case of transient droop functions (2) and transient and steady-state droop functions, (2) and (3), for the purely converter based local distribution system.

Fig. 8 shows detailed results of the low-pass filtered AC side voltage for a switch-mode model simulation and small-signal model simulation for f_s=6.0 kHz and f_s=10.0 kHz. The small-signal, state-space model is simulated in SIMULINK™ and the simulated model is the same as the one used to create Fig. 5 and Fig. 6. The switch-mode model simulation result is the same as shown in Fig. 7 for the case with both transient and steady-state droop functions. The previously announced problem with the small-signal model in case of low sampling frequency is apparent from Fig. 8.

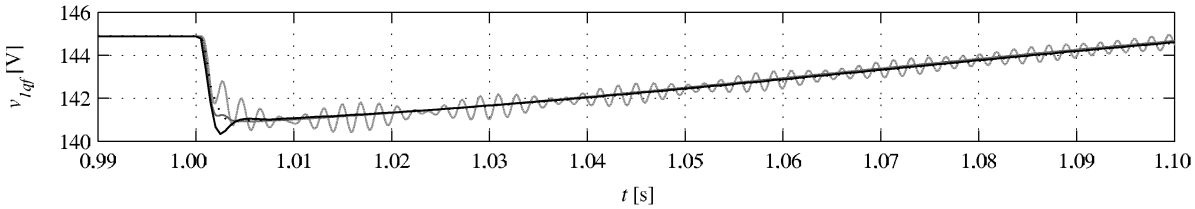

Fig. 8: Unit 1 low-pass filtered output voltage v_{1qf} of the switch-mode simulation model (*black*) for f_s=10.0 kHz (solid) and f_s=6.0 kHz (dotted) and state-space simulation model v_{1qf} for f_s=6.0 kHz (*light-grey*) and f_s=10.0 kHz (*dark-grey*) in the case of a load converter active power reference (p_3^*) increase of -0.5 pu (-3750 W) at t=1.0 s. Both transient (2) and steady-state (3) droop functions are implemented in the source converters of these simulation models.

In the previously shown simulation results the distributed power system is mainly resistive. To investigate the impact of a mainly inductive grid X/R is increased to 10 while the impedance Z is maintained. Simulation results for this case are shown in Fig. 9. From Fig. 9 it is obvious that power quality is not degraded in this case. Still, in the case of line inductance in the same order of magnitude as the converter output filter inductance there can be a considerable degradation of power quality in terms of voltage disturbance. The origin of this degradation is the LC-circuit formed by the line inductance and the converter AC side capacitors. Also, the switching frequency voltage ripple is divided between the converter output filter inductance and the line inductance. The dynamical properties and load sharing are not affected by this increased X/R ratio. Only the grid voltage is shown in Fig. 9 since the other quantities are essentially equal to the ones presented in Fig. 7.

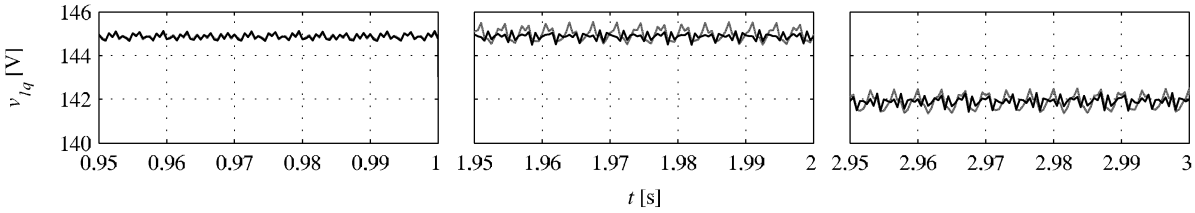

Fig. 9: Simulated converter 1 voltage v_{1q} in the case of cable segments with X/R=10 (*black*) and X/R=0.1 (*grey*) for total impedance of each cable segment of Z=0.1 Ω at a load converter active power reference (p_3^*) increase of -0.5 pu (-3750 W) at t=1.0 s and reactive power reference (q_3^*) increase of -0.5 pu (-3750 VAr) at t=2.0 s.

Now a rotating generator, in this case a synchronous machine, is included in the system to model a generator directly connected to the grid, i.e. without power electronic interface, in the middle of the cable segment connecting converters 1 and 3. The rotating power source is also controlled to deliver active and reactive power according to the droop functions (3). The rotating generator affects the

system behaviour in the sense that the stationary load distribution is altered since the installed generating capacity increases. Fig. 10 shows the simulation results for the same load as shown in Fig. 7 but with the rotating generator included. The rated power of the rotating generator is 3.75 kVA and the inertia constant $H=5.0$ s. The dynamical behaviour of the system is slightly affected.

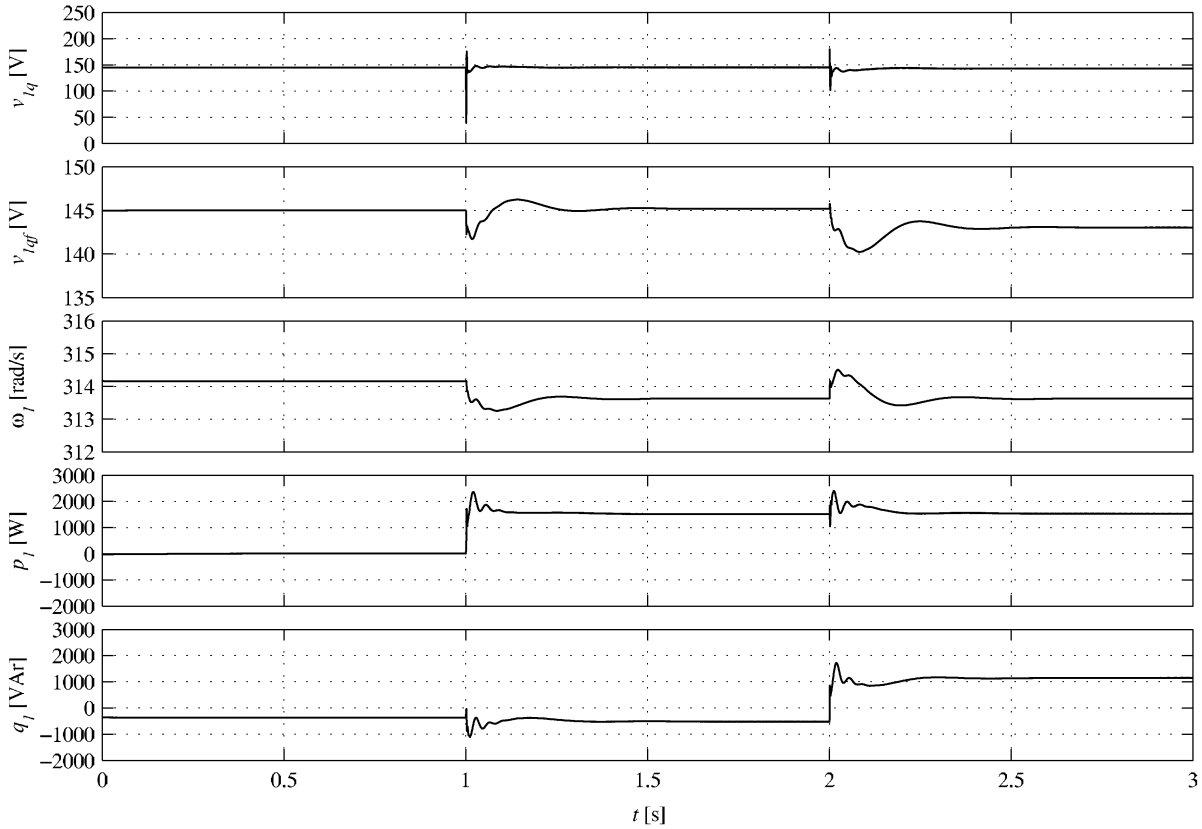

Fig. 10: Switch-mode model simulation results in the case of a load converter active power reference (p_3^*) increase of -0.5 pu (-3750 W) at $t=1.0$ s and a load converter reactive power reference (q_3^*) increase of -0.5 pu (-3750 VAr) at $t=2.0$ s. Note that a rotating generator is included in the system which require that both transient (2) and steady-state (3) droop functions are implemented in the source converters of this simulation model.

Experimental results

The investigated system is verfied in laboratory experiments. The same converter parameters as used for the simulations are used also in the experimental investigation of a three-converter system without rotating generators and external AC network. To model the impedance of a three-phase cable, series resistors (0.1 Ω per phase) are connected between each converter. The resistors are rated 5 W and therefore lower load than used in the previous simulations is investigated (0.25 pu). The controllers are implemented in DSpace^{TM} with sampling frequency $f_s=10.0$ kHz since the laboratory equipment is for general purpose and, as such, not equipped with adequate anti-aliasing filters. Both switch-mode simulation and experimental results for converter 1 are shown in Fig. 11. As shown in Fig. 11 there is a high degree of agreement between simulation and experimental results. There is a slight difference between simulated and measured reactive power, which is likely due to a difference between rated and actual capacitance of the AC side capacitors. Also, the actual impedance of the network is most likely not accurately modeled. Both active and reactive load-sharing operates properly considering the high impedance. The active power supplied by converter 1 (p_1) is 0.011, 0.253 and 0.278 pu (unit base) and the reactive power (q_1) is -0.040, -0.053 and 0.144 (unit base) at time instants (t) 0.5, 1.5 and 2.5 s, according to Fig. 11. The corresponding loading of source converter 2 is (p_2) 0.010, 0.273 and 0.277 pu (unit base) and (q_2) -0.073, -0.003 and 0.223 pu (unit base).

 ISBN : 90-75815-08-5

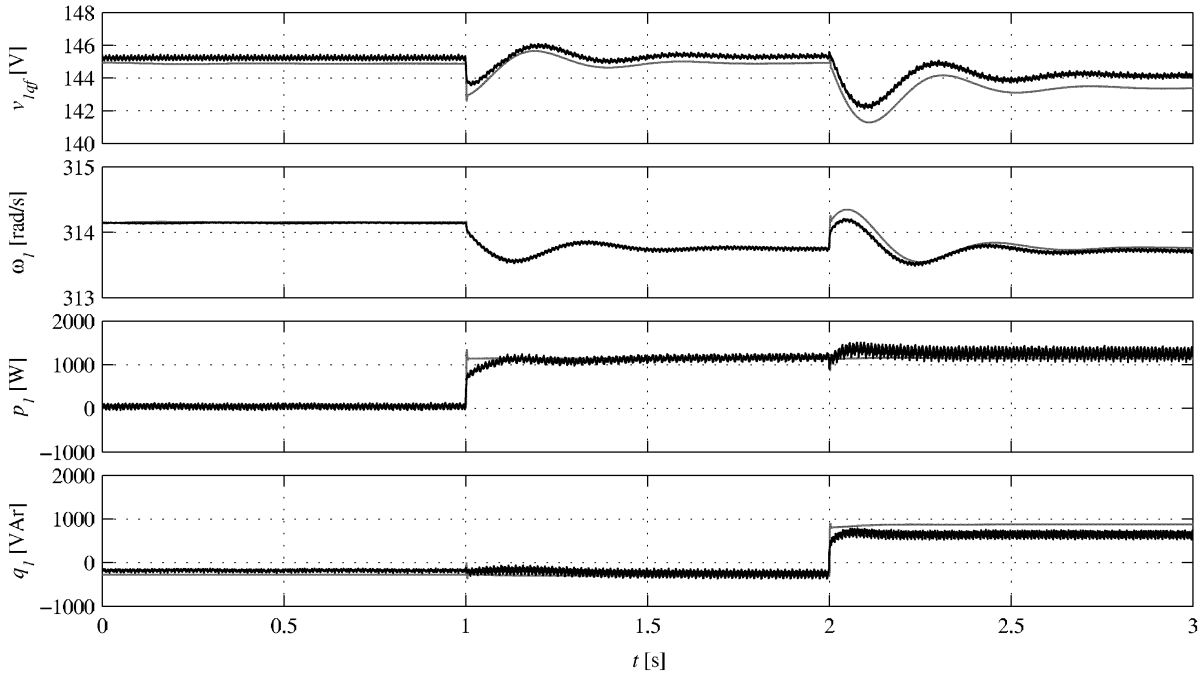

Fig. 11: Experimental (*black*) and simulation (*grey*) results for converter 1 (source) in the case of a load converter active power reference (p_3^*) increase of -0.25 pu (-1875 W) at $t=1.0$ s and a reactive power reference (q_3^*) increase of -0.25 pu (-1875 VAr) at $t=2.0$ s. Transient (2) and steady-state (3) droop functions are implemented in the source converters.

Conclusions

In this paper stability and dynamic properties of an AC distributed generation system are investigated. It is found that the presented voltage and frequency droop controllers of the power electronic converters operate satisfactory in both stand-alone mode and when rotating sources are included in the distributed generation system, in the case of constant power loads. The results are verified in simulations and the stand-alone capability is verified also in experiments. Load-sharing is acceptable for the investigated, highly resistive, network. Power quality, load-sharing and dynamical properties are not affected when X/R of the cable segments is increased from 0.1 to 10 for $Z=0.1$ Ω.

References

[1]. M.C. Chandorkar, D.M. Divan and R. Adapa, "Control of Parallel Connected Inverters in Standalone AC Supply Systems", *IEEE trans. Industry Applications*, vol. 29, no. 1, pp. 136-143, Jan./Feb. 1993.

[2]. R. Tirumala, N. Mohan and C. Henze, "Seamless Transfer of Grid-Connected PWM Inverters Between Utility-Interactive and Stand-Alone Modes", *IEEE APEC 2002 Conf. Proc.*, Dallas, Texas, Mar. 10-14, 2002, pp. 1081-1086.

[3]. Y. Li, M. Vilathgamuwa and P.C. Loh, "Design, Analysis, and Real-Time Testing of a Controller for Multibus Microgrid System", *IEEE trans. Power Electronics*, vol. 19, no. 5, pp. 1195-1204, Sept. 2004.

[4]. S. Wijnbergen and S.W.H. de Haan, "Power Electronic Interface with Independent Active and Reactive Power Control for Dispersed Generators to Support Grid Voltage and Frequency Stability", *EPE 2003 Conf. Proc.*, Toulouse, France, Sept. 2-4, 2003, CD-ROM pages 8.

[5]. A. Engler, "Applicability of Droops in Low Voltage Grids", *International Journal of Distributed Energy Resources*, vol. 1, no. 1, pp. 3-15, Jan.-Mar. 2005.

[6]. P. Karlsson, "Small-Signal Modeling and Analysis of DC Distributed Power Systems", *NORPIE 2004 Workshop Proc.*, Trondheim, Norway, June 14-16, 2004, *(CD ROM pages 6).*

[7]. L. Harnefors and H.-P. Nee, "A General Algorithm for Speed and Position Estimation of AC Motors", *IEEE trans. Industrial Electronics*, vol. 47, no. 1, pp. 77-83, Feb. 2000.